NINETEENTH EUROPEAN ROTORCRAFT FORUM

PAPER N. G16

ANISOTROPIC ROTOR STABILITY

By

N.S. PAVLENKO
MIL MOSCOW HELICOPTER PLANT
MOSCOW, RUSSIA

September 14-16, 1993
CERNOBBIO (COMO)
ITALY

ASSOCIAZIONE INDUSTRIE AEROSPAZIALI
ASSOCIAZIONE ITALIANA DI AERONAUTICA ED ASTRONAUTICA

ANISOTROPIC ROTOR STABILITY

N.S. Pavlenko

Mil Moscow Helicopter Plant
Moscow, Russia

ABSTRACT

The paper describes the technique used for analysis of the helicopter main and tail rotor stability. The technique provides for determination of the required flutter and divergence margns for a helicopter in level flight, as well the ground resonance margin for a helicopter with an anisotropic rotor. Small oscillations of the rotor mounted on a flexible support are described by a homogeneous system of linear differential equations with periodic coefficients. The stability of the system solutions is investigated with the use of the Floquet theory.

The effect of the reduced damping ability or a complete failure of the drag hinge damper of one of the blades on the stability of the rotor as a whole is considered when analyzing a single-rotor helicopter for ground resonance.

The boundaries of the area of instability experienced by the two-bladed tail rotor of the Mi-34 helicopter are established. The effect of various parameters on the position and extension of the instability area has been analyzed. Experimental data confirming the analysis results are given.

Some results obtained from the stability analysis of a tilt rotor designed for the tilt-rotor aircraft are cited.

INTRODUCTION

The advent of a new generation of helicopters, such as the Mi-28 and Mi-34, has been feasible owing to application of composite materials and new blade and hub designs of the main and tail rotors (Figs. 1 and 2). These helicopters made loops and rolls: the Mi-34 in 1988, and the Mi-28 in 1993.

When designing the main rotor of the Mi-28, a high-speed maneuverable combat helicopter, the glass-fibre plastic blades and the hub incorporating elastomeric bearings were used for the main blades. The flapping, drag and feathering hinges were replaced by a common spherical elastomeric hinge ensuring all required motions of the blade. New airfoil types providing improved performance were used for the main rotor blades.

The process of obtaining the Mi-28 high performance was accompanied by problems which had to be solved at once. For instance, a peculiar feature of the new main rotor blades was an intensive growth of the cosine component of the first harmonic of the hinge moment with the increase of the airspeed leading to a higher level of moments acting on the swashplate. This resulted in a considerable increase (with the airspeed) of the total constant moments on the swashplate in contrast to the

blades of the Mi-24 helicopter whereon these moments changed but slightly with the increase of the airspeed and showed a general tendency towards their decrease.

A development programme carried out in the course of the tests and including the selection of the rational shape of the blade tip, root and trailing edge has allowed to reduce control loads.

Oscillatory instability of the main rotor occurred in the flying test bed (the Mi-24) was another complicated problem, the blade airfoil chordwise oscillations with a frequency close to that of the first overtone of the blade natural oscillations being the highest. The occurrence of this kind of instability is explained both by general factors typical of the Mi-28 main rotor blades and hub, as well as by specific features associated with the adaptation of the new rotor system to the Mi-24 helicopter used as a flying laboratory.

The general factors include development of relatively light-weight blades, as compared with those of the Mi-24 helicopter, due to application of composite materials. The specific features include unfavourable pitch-lag coupling and a sharp decrease of the damping ability of the drag hinge damper of one of the blades because of seal leakage. To define the appropriate margins till the onset of flutter and ground resonance, account should be taken of the reduced damping ability of individual dampers due to their partial or complete failure as well as to a wide spread in springy and damping properties.

Small oscillations of the rotor mounted on a flexible support are described by a homogeneous system of linear differential equations with periodic coefficients. The periodicity of the system coefficients involves some difficulties in the determination of the system solution stability.

However, it is not possible to obviate the periodic coefficients in the above-mentioned cases and in the analysis of stability of a two-bladed rotor mounted on the anisotropic flexible support when the elastic or damping parameters of the support are different in two mutually perpendicular directions. The need for such an analysis was felt when the two-bladed tail rotor of the Mi-34 helicopter showed instability. It should be noted that any kind of flutter of the rotating rotor encountered in helicopter level flight is also described by a system of differential equations containing periodic coefficients.

The present paper describes a method which can be used for calculating flutter margins for helicopters in level flight, as well as divergence and ground resonance margins. The method is based on investigations into stability of systems of differential equations containing periodic equations.

METHOD USED FOR ANALYSIS

Equations describing rotor oscillations can be written in the following form:

$$A(t)\ddot{q} + B(t)\dot{q} + C(t)q = 0 \qquad (1)$$

where: $q(t)$ is column matrix of the generalized coordinates;
$\dot{q}(t)$ and $\ddot{q}(t)$ are the first and second time derivatives of q;
$A(t)$, $B(t)$ and $C(t)$ are square matrices whose coefficients are periodic time functions in the general case.

Thus, expression (1) is a system of homogeneous linear differential equations of the second order with periodic coefficients.

Let us transform the system of equations (1) to its normal form by reducing its order. To this end, we introduce a column matrix containing new variables:

$$y^T = (q_1, q_2, \ldots q_m, \dot{q}_1, \dot{q}_2, \ldots \dot{q}_m),$$

where: $(\ )^T$ is the transposition operation.

After this transformation, the system of equations (1) can be written in the following form:

$$\dot{y} = G(t)y. \tag{2}$$

Here,

$$G(t) = \begin{pmatrix} 0 & E \\ -A^{-1}C & -A^{-1}B \end{pmatrix} \tag{3}$$

is a periodic matrix, E is a unit matrix.

Let us consider the fundamental matrix of Kochi solutions $Y(t)$ for the initial conditions:

$$Y(0) = E. \tag{4}$$

The value of $Y(t)$ at the end of the first period is called the monodromy matrix. The solution stability of equation (2) and hence of equation (1) fully depends on the properties of multipliers ρ_k which are the roots of the following equation:

$$\det [\ Y(T) - \rho E\ ] = 0. \tag{5}$$

Solutions of equation (1) are asymptotically stable if all multipliers are within a circle whose radius is a unity and are unstable if there are multipliers whose modulus is greater than a unity or there are $|\rho_k| > 1$.

The monodromy matrix can be calculated by various methods. The most frequently used technique consists in integrating the system of equations (2) by using one of the numerical methods [2]. In this case, the Kochi problem is solved 2m times over the interval $[0, T]$ for initial conditions (4). Each solution forms a column of the monodromy matrix. The success of this method depends on the selection of the numerical algorithm for solving differential equations. When solving the problems associated with investigations into stability of the main and tail rotor blade oscillations, it often happens that it is difficult to select the appropriate integration method since the required accuracy of calculations cannot be attained at any

integration step.

Another frequently used technique is the method of successive approximations [3, 4] when the solution of the system of equations (2) with periodic coefficients is represented in the form of an integral:

$$y(t) = y_0 + \int_0^T G(t)ydt, \qquad (6)$$

where: y_0 means the initial conditions.

Assuming a certain appoximation as an initial condition and repeating calculations from formula (6) m times, we can find the expression determining Y(t):

$$y(0,T) = y_0 [\, E + \int_0^T G(t)dt + \int_0^T G(t) \int_0^T G(t)dtdt + \ldots$$
$$\ldots + \int_0^T G(t) \int_0^T G(t) \int_0^T G(t) \ldots \int_0^T G(t)dtdtdt \ldots dt] \qquad (7)$$

Using Y for denoting the expression given in the square brackets, we have:

$$Y = E + \int_0^T G(t)dt + \int_0^T G(t) \int_0^T G(t)dtdt + \ldots$$
$$\ldots + \int_0^T G(t) \int_0^T G(t) \int_0^T G(t) \ldots \int_0^T G(t)dtdtdt \ldots dt \qquad (8)$$

Here: Y is a constant matrix, or a monodromy matrix.

For most of the problems related to rotor dynamics, it is unrealizable to calculate the monodromy matrix from formula (8) owing to the complexity of the integrals contained in the right-hand part of the formula. Therefore, the interval [0, T] is divided into 2m number of equal smaller intervals t, and in each smaller interval periodic matrix G(t) is replaced by constant matrix $G_к$:

$$G(t) \approx G_к = \text{const}.$$

Using solution continuity of the system of equations at the division points, the formula for calculating the monodromy matrix in the form of the product of exponential matrix functions is obtained:

$$Y(0,T) = \exp[(\, T - t_{m-1})G_{m-1}] \exp[(\, t_{m-1} - t_{m-2})G_{m-2}] \ldots$$
$$\ldots \exp[(\, t_1 - t_0)G_0].$$

This method was used by V.M. Pchelkin to analyze pitch-lag instability. Replacement of time variable matrix G(t) with constant matrix $G_к$ will cause an error which can spoil the result of the monodromy matrix calculations.

To improve the accuracy of our calculations, the following technique is used in the given paper. The interval solutions are

presented by the periodic matrices G(t):

$$Y(0,T) = e^{\int_{t_{m-1}}^{T} G(t)dt} \cdot e^{\int_{t_{m-2}}^{t_{m-1}} G(t)dt} \cdot \ldots \cdot e^{\int_{t_0}^{t_1} G(t)dt} .$$

The matrix exponential is determined by using expansion into e power series.

The G(t) matrix integral is calculated by the Simpson method through the parabola approximation.

This presentation of the periodic matrix makes it possible to improve the accuracy of the calculation which is extremely important for the subsequent operation made in calculating the multipliers.

ANALYTICAL RESULTS FOR MULTIBLADED ROTORS

For ground resonance analysis, a single-rotor helicopter can be represented by a mechanical system called "the rotor on a flexible support" (Fig. 3) [1]. Absolutely rigid blades are attached to the hub by the drag hinges comprising damping devices and springs simulating the elastic properties of the blades.

The hub is connected to the shaft rotating in the bearing supports of the casing having mass M. The casing has two degrees of freedom, X and Z, corresponding to its in-plane displacement, and is attached by the dampers and springs to a fixed support. The elastic and damping characteristics of the support and the blades are considered to be linear and proportional to the support and blade displacement and speeds, respectively. Spring rates of the blades in the drag hinges of the hub are not equal. Likewise, the dampers can differ from one another. The frequencies of the support natural oscillations in directions OX and OZ are not equal, and the damping coefficients for these directions are different as well. This is the way the anisotropic rotor mounted on the anisotropic flexible support is considered.

Stability of the anisotropic rotor was investigated in accordance with the procedure described above. The ground resonance analysis was made for a single-rotor helicopter having a five-bladed main rotor. Figure 4 illustrates the effect of reduced damping ability of the drag hinge damper of one of the rotor blades by 50 % and 90 %, as compared to the initial damping ability, on the critical damping value and on the width of the oscillatory instability area which is characteristic of multibladed rotors. One of the curves in the figure corresponds to a complete failure of the damper of one of the blades. The relative speed of the rotor $\bar{\omega} = \omega / P_x$ is plotted on the X-axis, and the blade relative damping $\bar{n} = n / P_x$, on the Y-axis.

The charts are given for the support relative damping when the oscillations in direction OX equal $\bar{n}_x = n_x / P_x = 0.2$ and those in direction OZ, $\bar{n}_z = n_z / P_x = 0.25$. It is clear from the charts that a deterioration of the characteristics of at least one blade damper considerably reduces stability of the

whole system. If one of the dampers fails completely, the instability area cannot be limited even if the damping coefficients of the other blade dampers have very great values.

ANALYTICAL RESULTS FOR TWO-BLADED ROTORS

During the Mi-34 flight tests high alternating stresses in the two-bladed tail rotor shaft were registered. The amplitude of the alternating stresses measured in various flights was unstable and reached +105 MPa. In this connection, the areas of instability of the tail rotor mounted on a flexible support were calculated (with allowance for the flexibility of the shaft, tail rotor gearbox and tail boom).

For calculations, it was assumed that the in-plane natural frequency of the non-rotating blade was $P_\zeta = 1.6\omega$. The flexible support frequencies determined experimentally were equal to Px = 320 rad/sec and Pz = 307 rad/sec. Thus, it was the case of the anisotropic support wherein the system of equations (1) could not be transformed into an equivalent one containing coefficient constant matrices.

From the calculations the area of aperiodic instability (Fig. 5) was obtained, wherein a pair of the complex-conjugate roots extended over the real axis and subsequently moved along this axis in opposite directions with one of the roots going beyond the limits of the circumference whose radius is equal to unity. The imaginary part of the multiplier turned to be equal to zero (Fig. 6).

In this case, critical oscillations of the rotating shaft occur, when the centre of gravity of the oscillating blades is offset, and the resulting out-of-balance makes the hub oscillate at a frequency equal to the rotor speed in the non-rotating coordinate system. Here combination frequencies with higher harmonics are likely to occur. Parametric calculations have been made to determine the effect of the main parameters of the tail rotor-shaft-tail boom system on the position and extension of the instability area. It is clear from the charts shown in Fig. 7 that the increased mass moment of blade inertia and higher in-plane natural frequency of the blade result in improved stability. In accordance with the calculations, the increased damping ability of the support improves rotor stability too.

The results of the calculations for various support frequencies are shown in Fig. 8. It is evident from the figure that this kind of instability occurs when the rotor angular speed is close to one of the natural frequencies of the support.

The analysis of the results obtained has shown that various approaches can be used to remove the area of aperiodic instability from the rotor operational speed range. But the maximum efficiency is gained by changing the frequency characteristics of the support which make the instability area shift within the range of the rotor operational speeds.

The shifting of the instability area towards higher rotor speeds calls for the increased stiffness of the tail rotor-shaft-

tail boom system which, in its turn, results in a considerable increase of the mass of these units. The instability area can be shifted into the range of low rotor speeds by reducing the system stiffness which can be achieved by changing only one parameter, i.e. by increasing the length of the tail rotor shaft. The calculations have shown that, to shift the instability area to the tail rotor speed ω = 185 rad/sec, the shaft should be made 0.125 m longer. The new position of the aperiodic instability area for a longer tail rotor shaft is shown in Fig. 9.

TEST RESULTS

Based on the calculations performed, a longer tail rotor shaft was designed and manufactured, and the tail rotor comprising the new shaft was installed in the Mi-34 helicopter (Fig. 10).

Since the longer shaft had a longer arm and a reduced cross-sectional moment of inertia as compared to the initial version, the amplitude of the alternating normal stresses imposed by the rotor external loads should have become twice as large (for a stable operation of the rotor). But the test results showed that the elongation of the shaft had caused the reduction of the alternating stresses within the rotor operational speeds. The stresses had become greater at the rotor transient speed ω = 185 rad/sec whereto the instability area had shifted. At the same time, the tail unit vibration became noticeably lower.

Fig.11 illustrates the results of the Mi-34 tests for the tail rotor with both a short shaft and a long one. From the charts, it is clear that the alternating stress amplitude has reduced from 59 MPa to 13 MPa, i.e. it has become more than four times smaller.

ANALYSIS OF TILT ROTOR STABILITY FOR A TILT-ROTOR AIRCRAFT

The tilt rotor mounted on a flexible wing has been analyzed for stability in the course of R&D work on the tilt-rotor aircraft. The model which has been used for the analysis is shown in Figs. 12-14.

In this model, the blade is considered as a rigid body capable of flapping and lead-lag motions as well as torsional oscillations about its longitudinal axis. Spring rates C_{β_i} and C_{ζ_i} are selected so as to ensure the required frequency of the blade flapwise and chordwise natural oscillations. The hub design is shown in Fig. 14. The hub can execute angular displacements φ_x and φ_z about the centre of the sphere (point O in Fig.14). The blade pitch control system comprises the cyclic and collective pitch control channels: φ_{x1}, φ_{z1}, and φ_0.

To describe linear displacements of the engine nacelle mounted on a flexible wing, designations X_1, Y_1 and Z_1 are introduced. Thus, the vector of the generalized coordinates

comprises seventeen components:

$$q^{T} = (X_1, Y_1, Z_1, \varphi_0, \varphi_{x1}, \varphi_{z1}, \varphi_x, \varphi_z, \beta_i, \varphi_i, \xi_i),$$

where: i is determined by the blade number. For a three-bladed rotor, its value varies from 1 to 3.

This paper presents the results of the first stage of the parametric calculations which have been made for the tilt rotor operating in the helicopter mode of flight. The system of the equations comprises two additional generalized coordinates shown in Fig. 15a (Fig. 15b illustrates another version of the control system).

The charts shown in Fig. 16 present the maximum modulus multiplier of the system of the equations versus the control linkage and swashplate stiffness. It is clear from the charts that any decrease in the control linkage and swashplate stiffness considerably reduces stability of the system.

There exist limit values of each of the parameters when the structure becomes unstable.

The charts shown in Fig. 17 illustrate the multiplier modulus versus the control linkage stiffness for various airspeeds. It follows from the analysis that, in level flight, instability of the system occurs at a greater value of the control linkage stiffness, i.e. the instability area is expanded.

The c.g. position also affects stability which is proved by the charts given in Fig. 18.

Thus, from the calculations,the effect of the tilt rotor main parameters on stability of the tilt-rotor aircraft in the helicopter mode of flight has been obtained.

CONCLUSION

The suggested algorithm for the investigation of stability in solving linear systems containing second-order differential equations with periodic coefficients has proved its efficiency in the analysis of self-sustained oscillations of the helicopter main and tail rotors.

The ground resonance analysis of a single-rotor helicopter equipped with a five-bladed main rotor has shown that the decreased damping ability of the damper of one blade substantially reduces stability of the whole rotor.

The boundaries of the aperiodic instability area have been determined for the Mi-34 two-bladed tail rotor. The recommendations to redesign the tail rotor have been given on the basis of the calculations. These recommendations provide for the shifting of the instability area from the rotor operational speeds into the range of rotor transient speeds. In the resulting modification, the alternating stresses in the tail rotor components have been reduced to the values ensuring the required service life of the tail rotor.

Some data have been obtained on stability of a tilt rotor designed for the tilt-rotor aircraft.

REFERENCES

1. Mil M.L., Nekrasov A.V., Braverman A.S., Grodko L.N., Leikand M.A. Helicopters, book 2. Oscillations and dynamic strength. Moscow, 1967.

2. Bolotin V.V. Numerical analysis of stability of linear differential equations with periodic coefficients. In book: "Selected problem of applied mechanics", Moscow, VINITI Publishers, 1974.

3. Erugin N.P. Reducible systems. Proceedings of the mathematical Institute of the Academy of Sciences of the USSR, XIII, 1946.

4. Bulgakov B.V. Oscillations, Moscow, GITL, 1954.

F I G U R E S

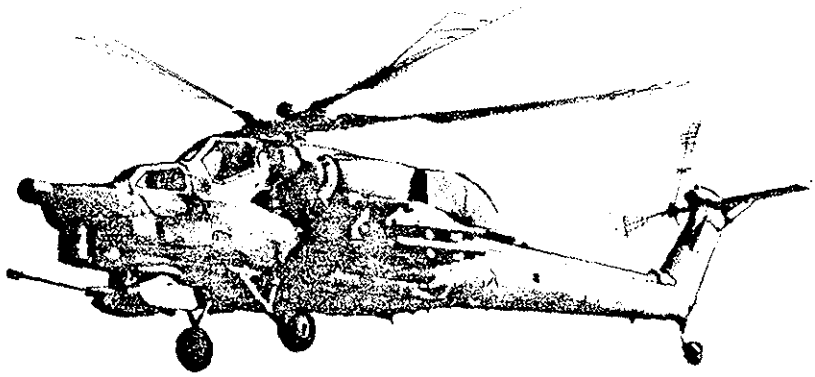

Fig. 1.

Mi-28 helicopter.

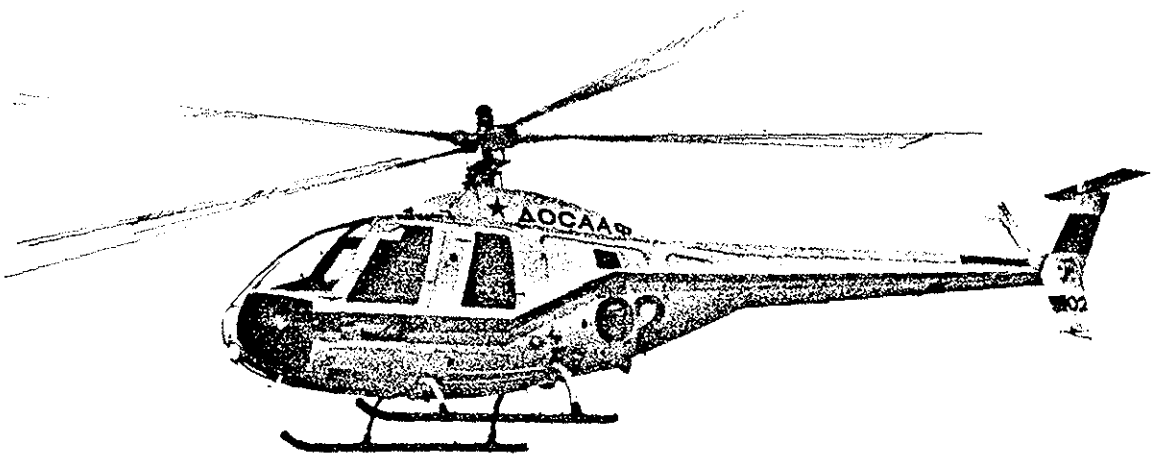

Fig. 2.

Mi-34 helicopter.

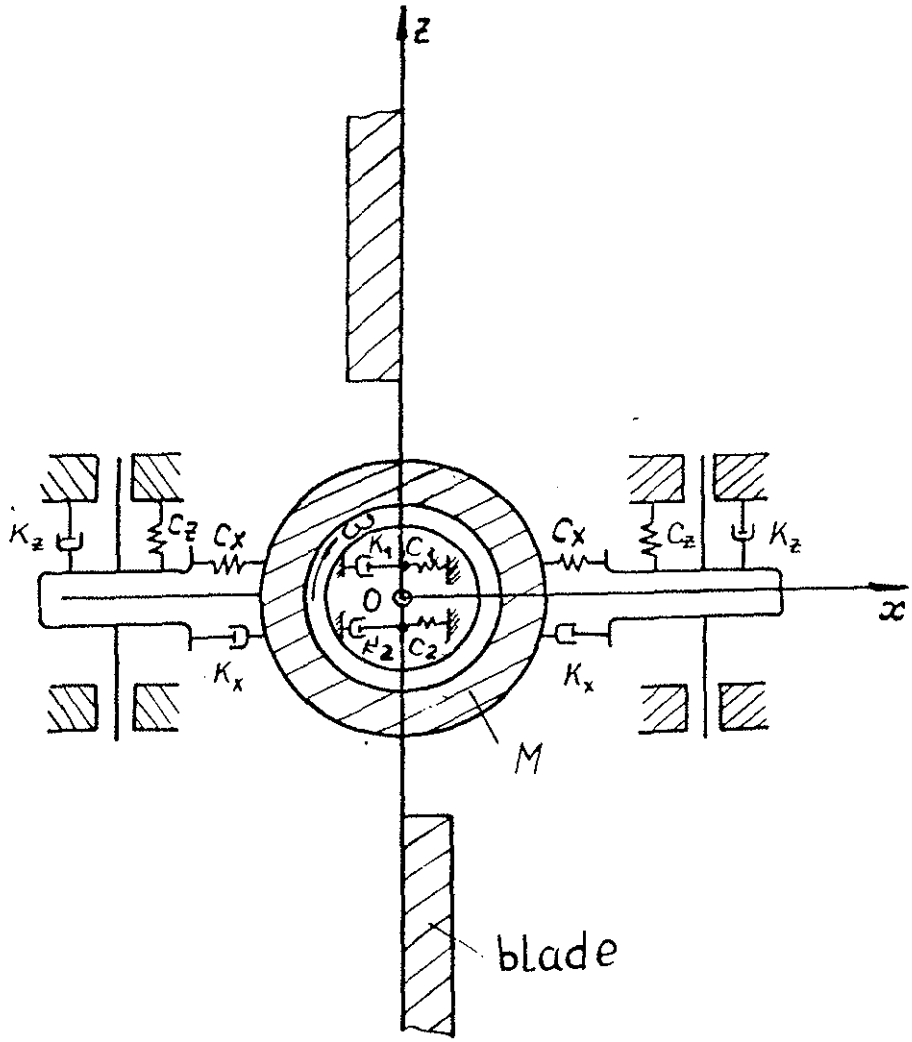
z
x
O
M
blade
K_z
C_z
C_x
K_1
C_1
K_2
C_2
K_x

Fig. 3.

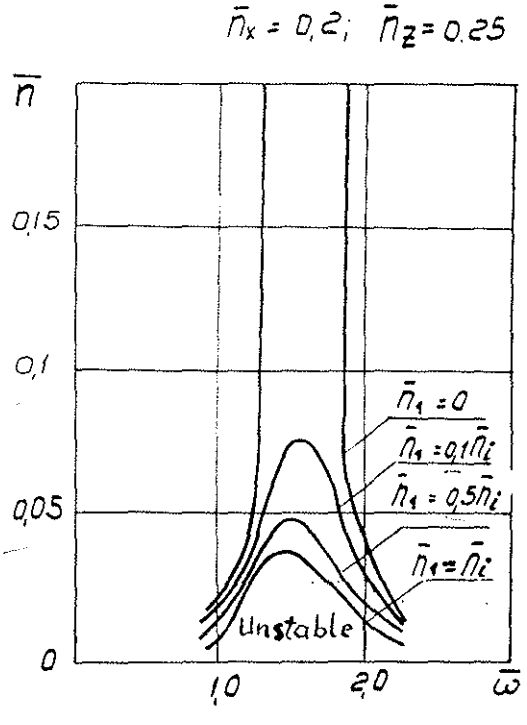
$\bar{n}_x = 0,2;\ \bar{n}_z = 0.25$
$\bar{n}$
0,15
0,1
0,05
0
1,0
2,0
$\bar{\omega}$
$\bar{n}_1 = 0$
$\bar{n}_1 = 0,1\bar{n}_i$
$\bar{n}_1 = 0,5\bar{n}_i$
$\bar{n}_1 = \bar{n}_i$
Unstable

Fig. 4.

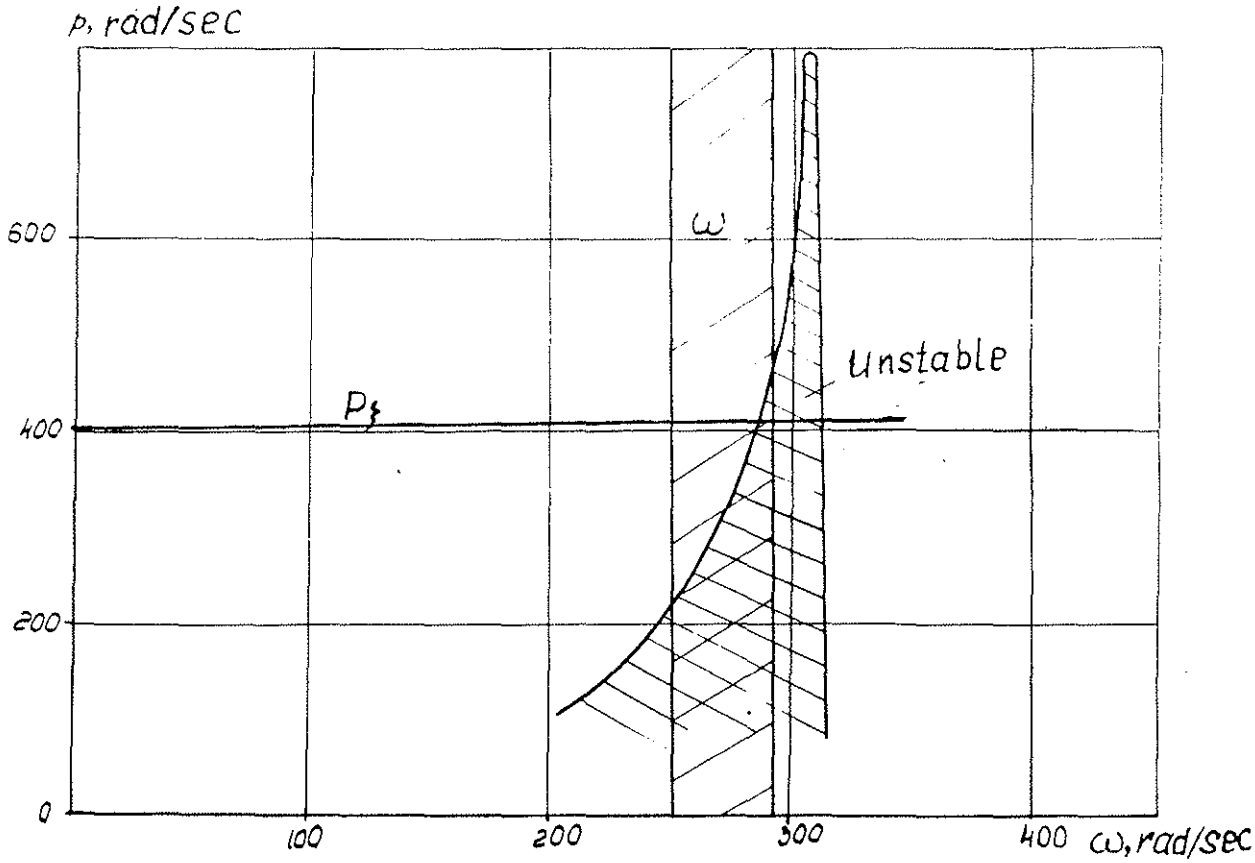
p, rad/sec
600
400
200
0
100
200
300
400
ω, rad/sec
ω
Unstable
P_ξ

Fig. 5.

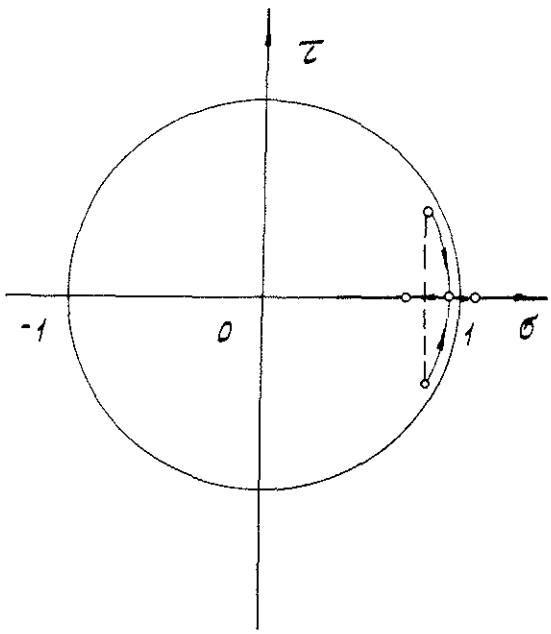
τ
-1
0
1
σ

Fig. 6.

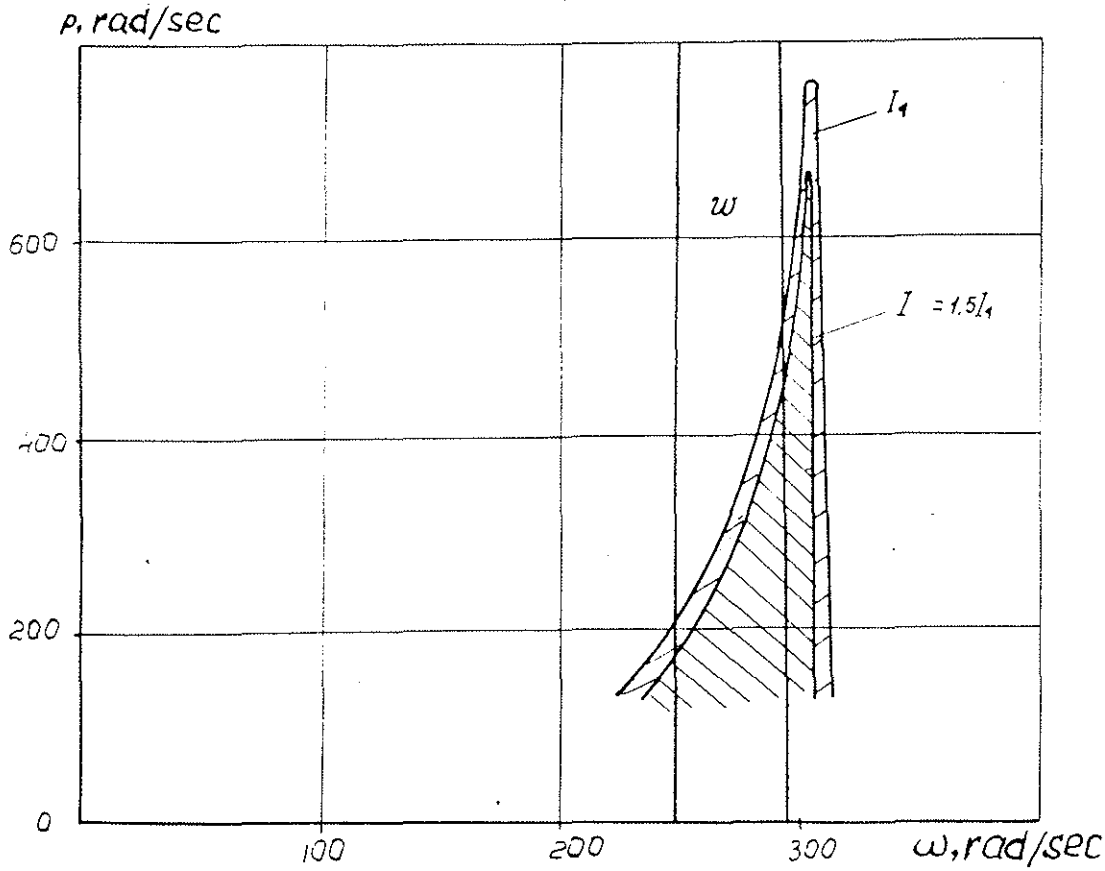
p, rad/sec
600
400
200
0
100
200
300
ω, rad/sec
w
I_1
$I = 1.5I_1$

Fig. 7.

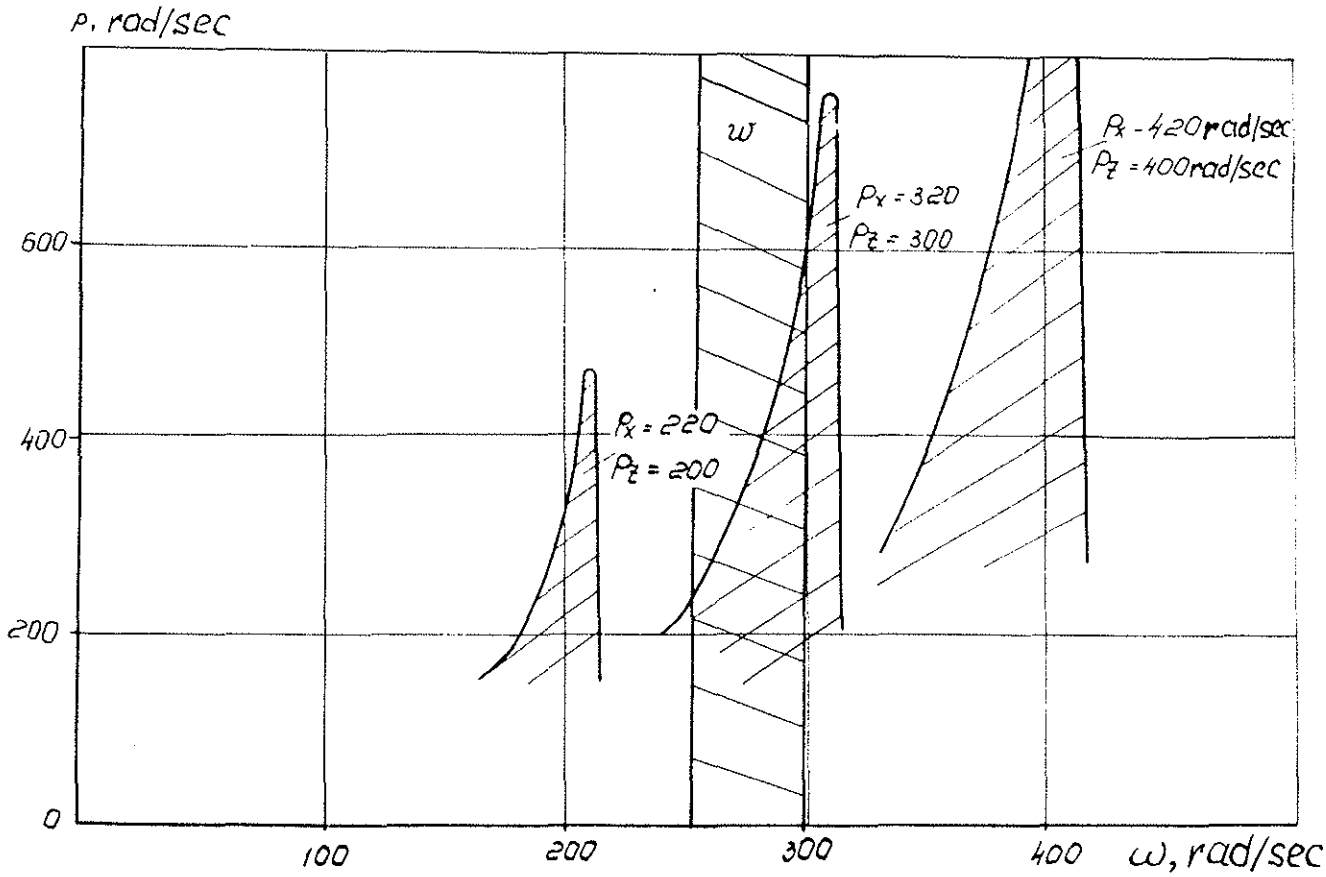
p, rad/sec
600
400
200
0
100
200
300
400
ω, rad/sec
w
P_x = 220
P_z = 200
P_x = 320
P_z = 300
P_x = 420 rad/sec
P_z = 400 rad/sec

Fig. 8.

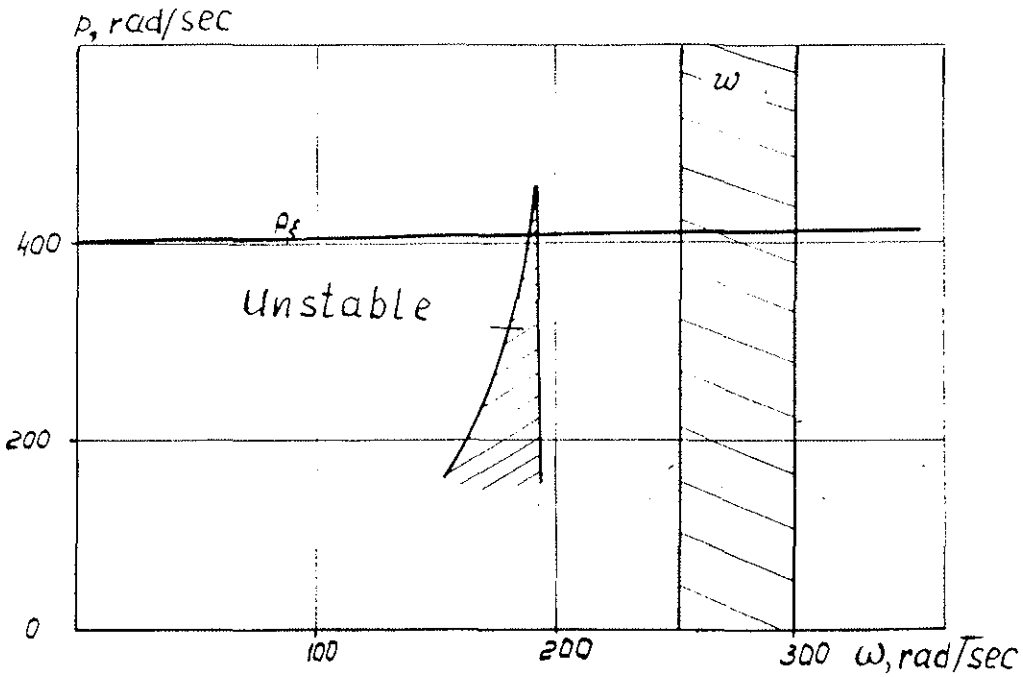
p, rad/sec
ω
400
200
0
Unstable
100
200
300
ω, rad/sec

Fig. 9.

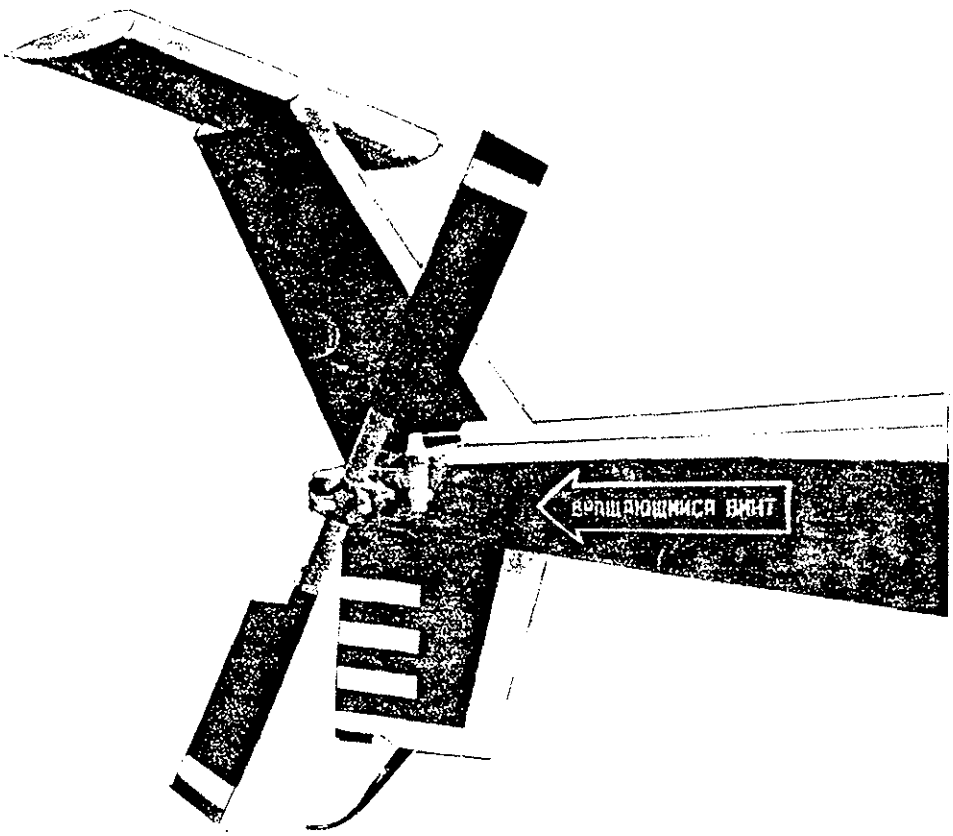
ВРАЩАЮЩИЙСЯ ВИНТ

Fig. 10.

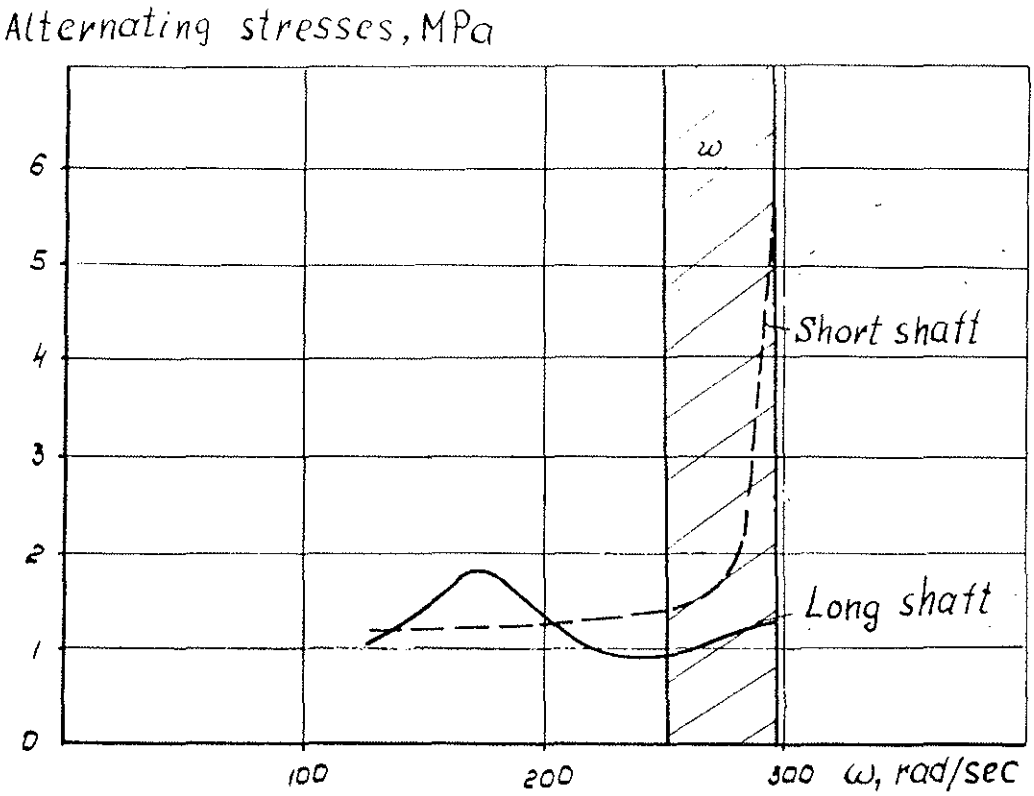
Alternating stresses, MPa
6
5
4
3
2
1
0
100
200
300
ω, rad/sec
ω
Short shaft
Long shaft

Fig. 11.

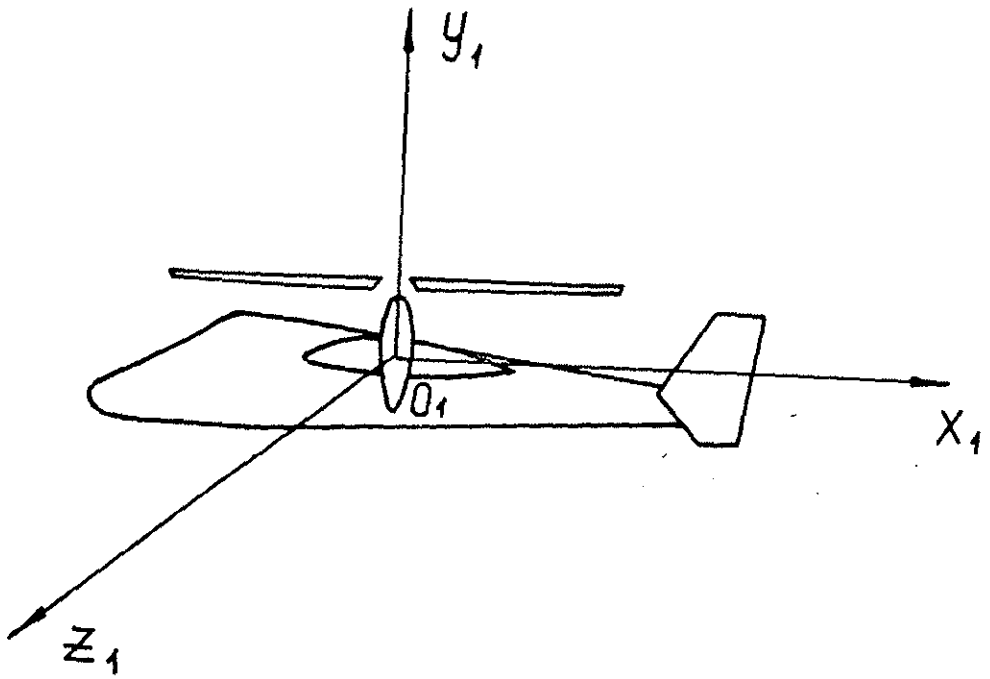
y_1
O_1
X_1
Z_1

Fig. 12.

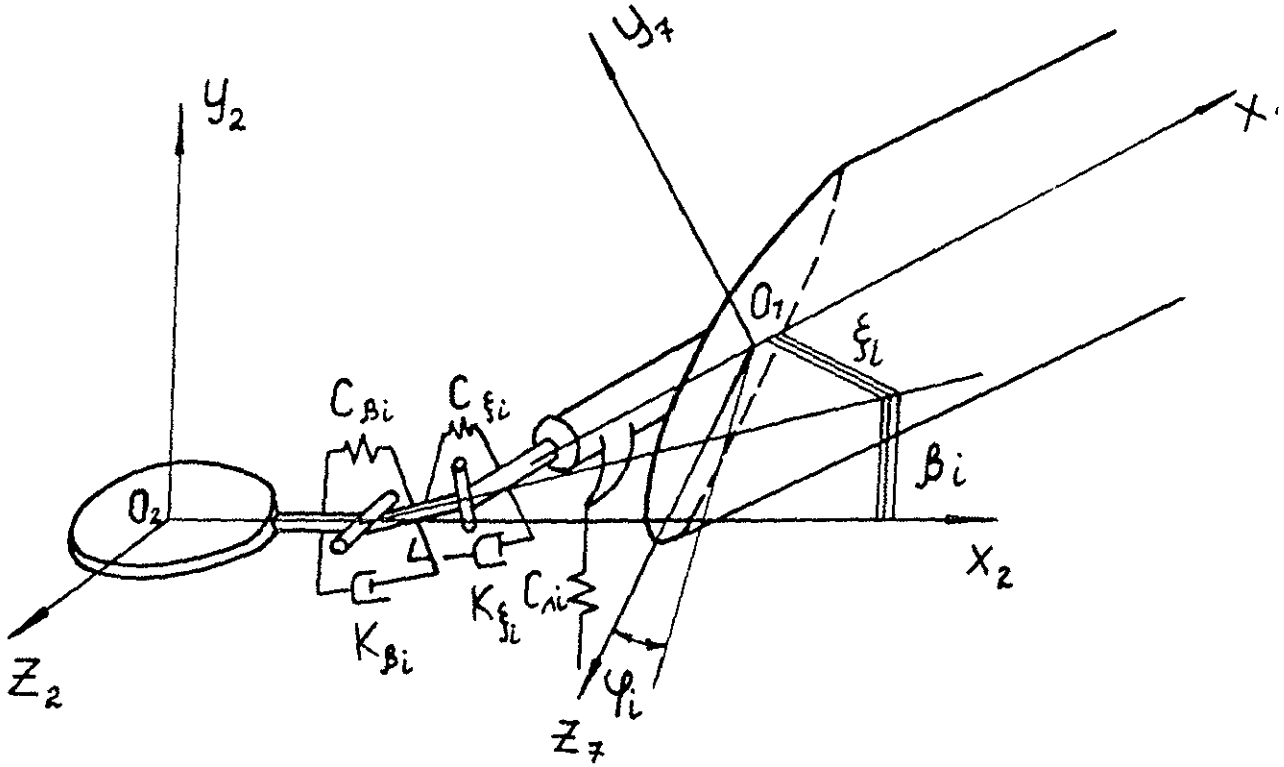
y_2
y_1
O_1
ξ_i
$C_{\beta i}$
$C_{\xi i}$
β_i
O_2
X_2
$K_{\xi i}$
$C_{\lambda i}$
$K_{\beta i}$
Z_2
φ_i
Z_1

Fig. 13.

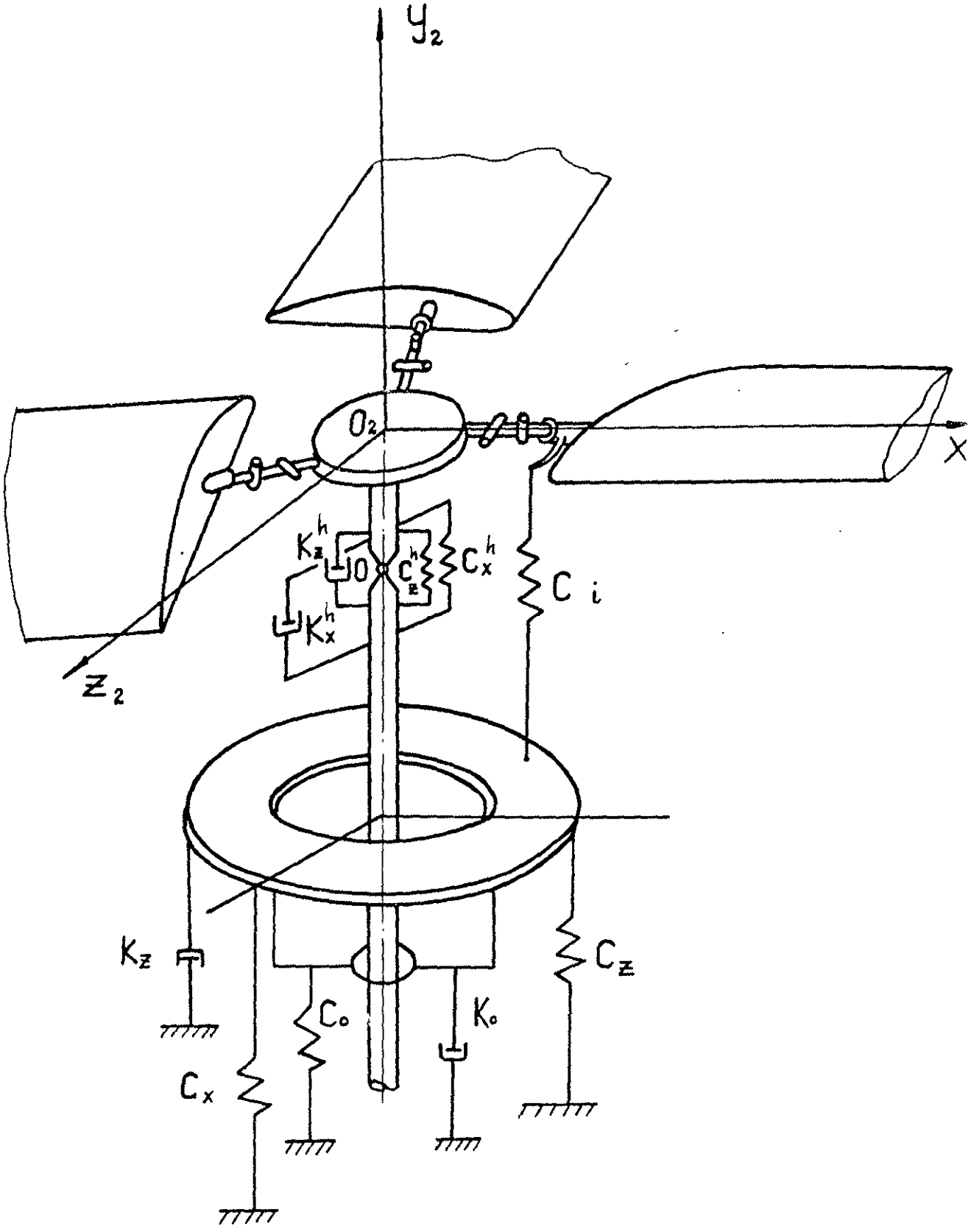

Fig. 14.

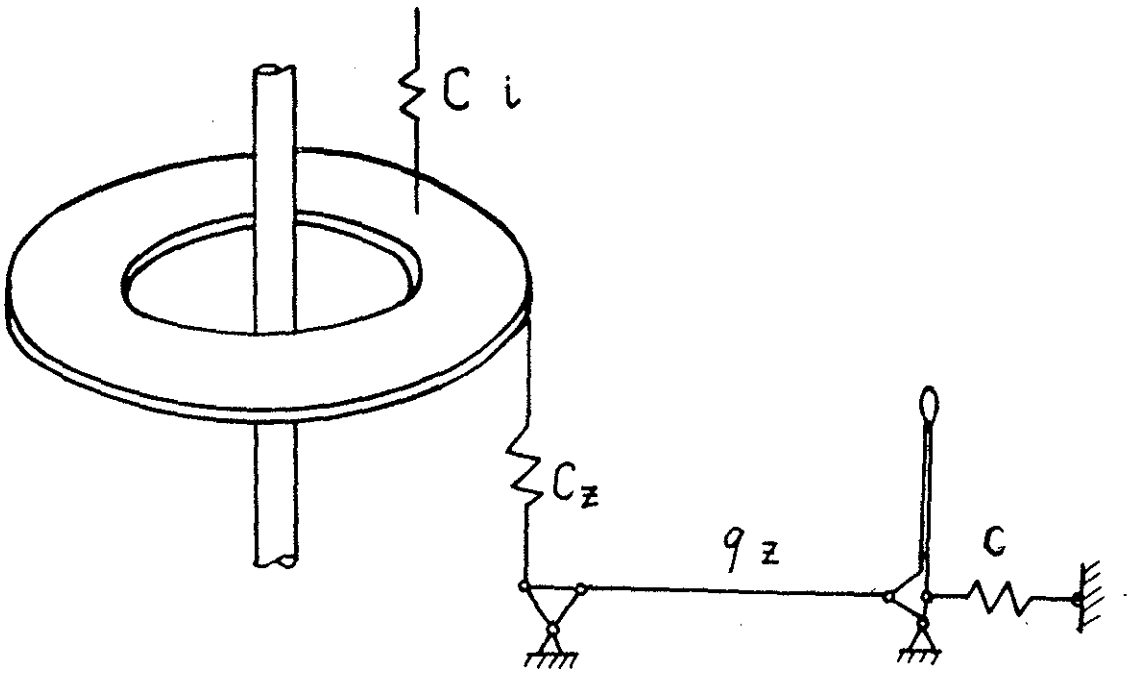

a) q_z (q_x) - linear displacements of rotor cyclic pitch control stick

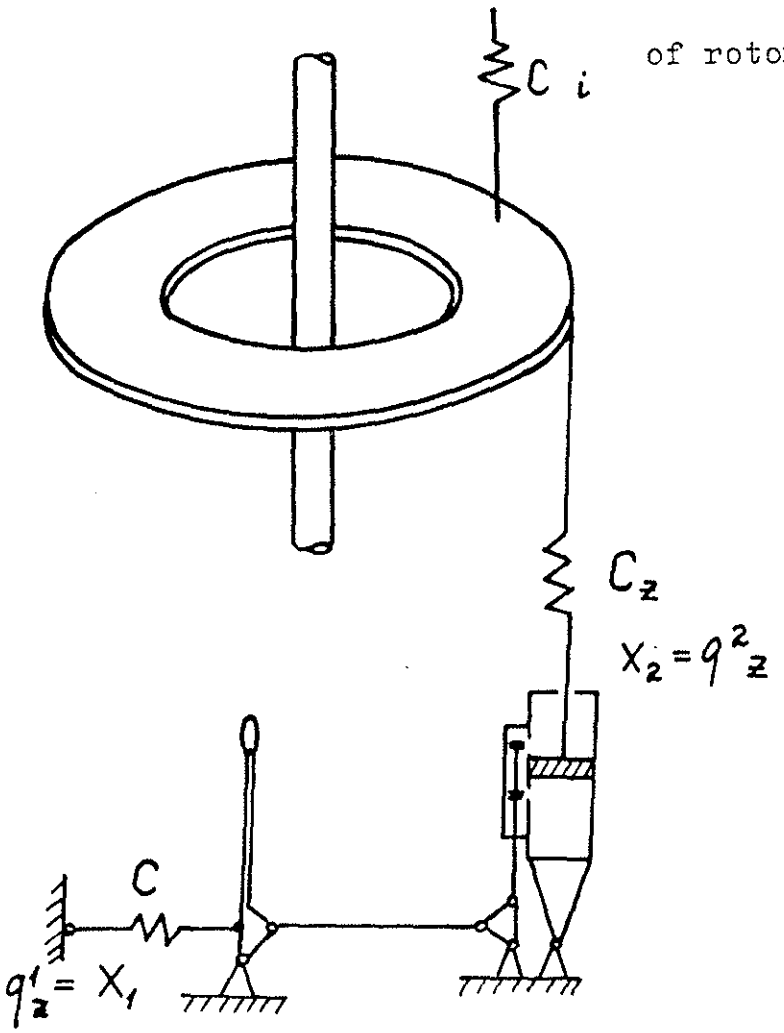

b)

Fig. 15.

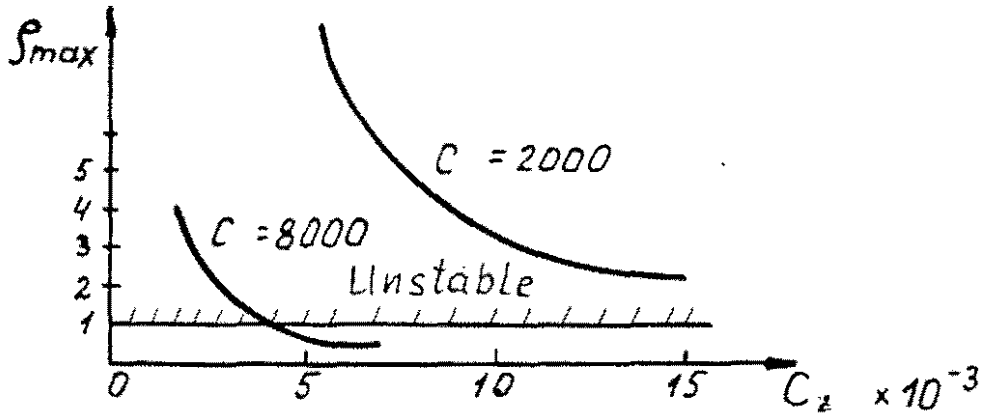

Fig. 16.

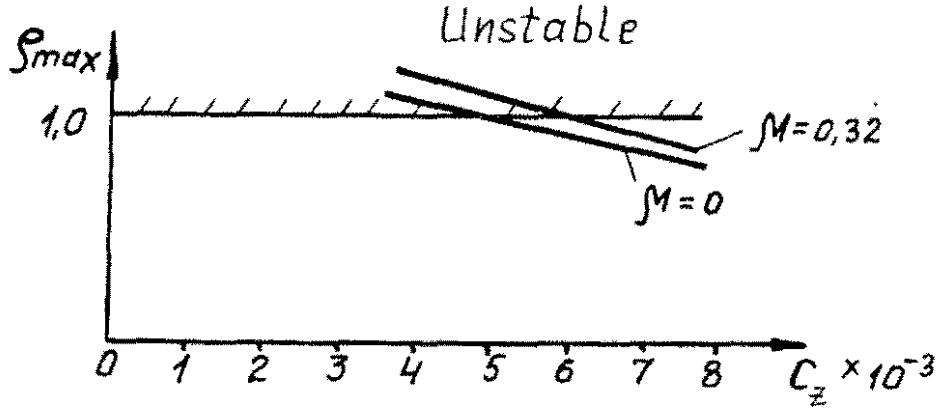

Fig. 17.

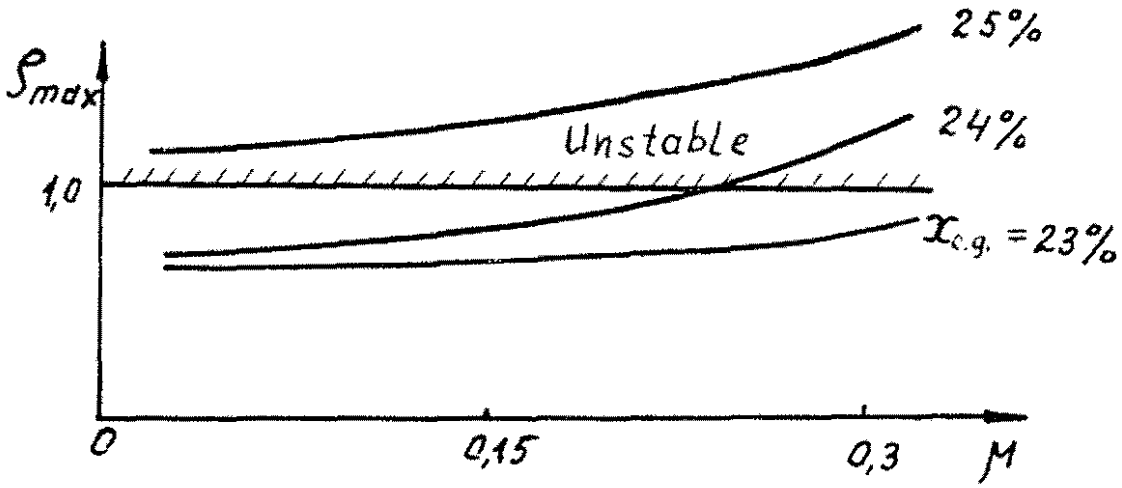

Fig. 18.